Supporting information for "Vulnerability of a semi-enclosed estuarine sea to ocean acidification in contrast with hypoxia"

Debby Ianson,[1,2] Susan E. Allen,[2] Benjamin L. Moore-Maley,[2] Sophia C. Johannessen[1] and Robie W. Macdonald[1]

Contents of this file

1. Text S1 to S4
2. Figures S1 to S2
3. Tables S1 to S6

Corresponding author: D. Ianson, Fisheries and Oceans Canada, Institute of Ocean Sciences 9860 West Saanich Rd, Sidney, BC V8L 4B2, CAN. (debby.ianson@dfo-mpo.gc.ca)

[1]Fisheries and Oceans Canada, Institute of Ocean Sciences, Sidney, British Columbia, CAN.

[2]Department of Earth, Ocean and Atmospheric Science, University of British Columbia, Vancouver, British Columbia, CAN.

Text S1.

Data Collection: The inorganic carbon system in the Straits of Georgia, Haro and Juan de Fuca was sampled in 2003, 2011 and 2012 (seven cruises) as part of an ongoing Fisheries and Oceans Canada (DFO) monitoring program in the region [*Masson*, 2006] and on a dedicated DFO OA survey in 2010 (Figure 1a; Table S1). Additional data were collected in the SoG during eight DFO mooring cruises during 2010 - 2012 [*Sutton et al.*, 2013] (Figure 1a; Table S1). Total alkalinity (TA) and dissolved inorganic carbon (DIC) were measured to define the carbonate system for each discrete sample (544 samples, with 12% replication). In addition to DIC and TA, discrete pH was measured on three cruises (Table S1). During all cruises full conductivity-temperature-depth profiles were collected. Dissolved oxygen (on-board Winkler titration with colorimetric endpoint detection, *Carpenter* 1965) and nutrient samples (nitrate, phosphate and silicic acid, $Si(OH)_4$); *Barwell-Clarke and Whitney* 1996) were collected from the same Niskin bottle as each discrete DIC/TA sample.

For all cruises except the OA survey (for which all samples were analyzed on-board), DIC/TA samples were placed in cool storage after collection and returned to the shore-based lab for analysis. DIC and TA collection and analysis followed standard protocol [*Dickson et al.*, 2007]. TA was analyzed using the open-cell system [*Dickson et al.*, 2007]. The spectrophotometric technique for pH analysis with purple m-cresol dye was used [*Clayton and Byrne*, 1993]. Salinity (S) is reported using the PSS-78 salinity definition [*UNESCO*, 1981].

Determining the carbonate system: To determine pH and Ω_a, TA and DIC (along with T, S, pressure (P), silicic acid and phosphate) were used with *Millero* [2010] constants and the standard CO2SYS [*van Heuven et al.*, 2011]. CO2SYS assumes that the calcium ion concentration [Ca^{2+}], necessary for estimating Ω_a, is controlled by S following *Riley and Tongudai* [1967]. We chose *Millero* [2010] because our data cover a large (low) range in S (5 - 34), and these constants agree with the *Millero* [1979] freshwater constants at S = 0.

Text S2.

Uncertainty estimation: These carbon data underwent careful quality control (see below). We estimated the standard deviation and pooled standard deviation (Sp) in replicate pairs to determine uncertainty due to sampling and analysis in DIC and TA. For samples analyzed onboard (summer 2010) the uncertainty was +/- 2 and +/- 4 μmol kg^{-1} for DIC and TA, respectively (>1000 total samples, most outside of this study region, with ~ 10% replication). For the majority of the samples (509 samples collected on 15 cruises, 12% replication) there appeared to be at least two populations of data. The differences between replicates for most pairs were within the range of uncertainty above (the 'good' data). However, the remaining replicate pairs had differences well outside of this range. Thus, uncertainty for all DIC and TA (excepting those collected on the single OA survey) is Sp; +/- 4 and +/- 10 μmol kg^{-1}, respectively. When individual replicate samples were subsampled for TA, the results were the same within +/- 2 μmol kg^{-1}, so the larger replicate differences are associated with sampling, not analysis. We suggest that these differences result from a combination of stratification in the Niskin bottles, and a significant contribution of organics (in our case primarily acids, e.g. *Hunt et al.* [2011]) to TA. While the uncertainly in our data (especially in TA) is larger than in most open ocean data-sets, the signals in our data are larger still.

Quality control: Variations in DIC, TA, O_2, nutrients and pH (estimated and observed - pH_{obs} where available) with S were examined and contrasted. We consider our pH_{obs} to be precise, but not accurate. Therefore, the trends in pH_{obs} with S (on a single cast) are valuable in the quality control of DIC and TA.

1. If a DIC or TA datum fell away (> 40 μmol kg^{-1}) from the (first order) linear trend in S (e.g. Figure 2a) for a single cast (so isolated in time and space) **and** expected variation in biological variables was not observed (e.g. for a dubiously high DIC value, a low O_2, and high nutrient value is anticipated) then the datum was flagged.

2. If TA was less than its corresponding (unflagged) DIC S>20, then the TA was considered 'bad'.

3. If pH_{obs} was available and showed the same 'anomaly' within a cast as pH estimated from a flagged DIC and TA pair, then the flag was removed.

4. Finally all flagged data (from single casts) were evaluated similarly (as in 1.) within the whole dataset. If a flagged datum fell within the range of values (at the same S) in the entire data set, the flag was removed and the datum considered 'good'.

Text S3.

Gas fluxes (CO_2 and O_2) in Haro Strait were calculated using the standard equations [*Wanninkhof et al.*, 2009], Schmidt number relationships [*Wanninkhof*, 1992], solubilities (CO_2 - *Weiss* 1974; O_2 - *Garcia and Gordon* 1992, 1993) and the *Ho et al.* [2006] gas exchange coefficient formulation. We used hourly wind speeds from Sandheads (in the S-SoG adjacent to the mouth of the Fraser River *Moore-Maley et al.* 2016; Figure 1a). These wind speeds were inflated by 1 m s^{-1} to account for the additional surface stress due to strong and consistent tidal currents in the region, increasing gas flux typically by 20%. The hourly fluxes were integrated over the 5 d residence time in Haro (R. Pawlowicz, pers. comm.) and multiplied by the region's surface area [1.23×10^9 m^2, *Riche and Pawlowicz* 2014] to obtain a total air-sea transfer of DIC and O_2 in the region corresponding to each sampling date.

Inventories of DIC and O_2 within Haro Strait (Inv_T) were estimated for each of the seven cruises (Table S3) that sampled Haro (Table S4) by linear interpolation between sampling depths. Only one Haro site was sampled per cruise. Contributions above the first sampling depth were determined using the slopes (e.g. dDIC/dz, where z is depth) derived from data from the top two depths. Contributions between bottom bottles and the seafloor were estimated by similar extrapolation. We multiplied water column inventory (mol m^{-2}) from the single site by the surface area of the Haro region [*Riche and Pawlowicz*, 2014] to obtain the total Haro inventory on each sampling date. This step assumes that water column inventories are the same throughout the region at any given time regardless of depth. While this assumption is not likely robust, six of the cruises sampled Haro at the same site, roughly the middle (deepest) location in the region (48.63°N, 123.24°W) allowing an unbiased comparison within this group.

The *disequilibrium* inventory was also estimated, i.e., amount of DIC that would need to be outgassed to return the entire water column to atmospheric P_{CO2} ($\mathrm{a}P_{\mathrm{CO2}}$) and the amount of O_2 that would need to be absorbed to bring O_2 to its equilibrium concentration at all depths (Inv$_d$, Table S4). Oxygen equilibrium (a function of T and S, *Garcia and Gordon* 1992, 1993) was calculated at each depth, allowing a water column inventory to be estimated as above (i.e. how much O_2 the water column could hold; Inv$_e$). We estimated the equilibrium DIC for each sampling depth associated with aP_{CO2} at the time of sampling and *in situ* measured TA, S, T, phosphate and silicic acid.

Text S4.

Determining summer DIC water mass end-members: DIC end-members associated with each of the four water masses influencing the S-SoG during summer [*Masson*, 2006], hereafter M06, were estimated. These water masses are; the sub-surface Pacific or deep JdF (*d*JdF), FR-plume which is in the surface S-SoG, deep S-SoG (*d*S-SoG) and deep N-SoG (*d*N-SoG) – (SW2, SW1, SW3 and SW5, respectively in M06). The deep water masses are easiest to consider. Because the DIC-S relationship is strong (Figure 2), we used the M06 S end-members (bold numbers in Table S5) to define each DIC end-member individually as follows. We took all the DIC data from the appropriate region in a tight S-envelope centred around the end-member S (S-range, Table S5). Each DIC datum was normalized (as below) to the M06 S to avoid potential bias if more data were available from one end of the S-range than the other, and the average was computed. Larger S-ranges were necessary where data were fewer (n, Table S5).

Normalization: Normalization of DIC at a given S to a specific salinity (Sn) is given by: DICn = (DIC - b)$\times$ Sn/S + b, where 'b' is the regionally specific DIC-intercept at S=0 [*Friis et al.*, 2003]. We considered the default case 'b'=0. We also estimated 'b' in each region from DIC-S data within that region. End-member calculation was not sensitive to 'b'. This lack of sensitivity was anticipated for the three deep water end-members because the salinity ranges were narrow (Table S5). The FR-plume end-member displayed greater sensitivity (results differed by 0.5%), however these results were within the standard deviation (std, Table S5) of the (normalized) data used. We present results from the 'b=0' default for all end-members.

FR-plume: The FR-plume, defined by M06 is a 'quasi end-member', associated with the upper 15 m of the water column at two sampling sites on the middle-west side of the S-SoG adjacent to the Fraser River (49.03° N 123.44° W and 49.16° N 123.55° W, Figure 1a). FR-plume is downstream of the pure FR-river end-member, which appears to be variable, and where sufficient data do not exist. To determine the DIC associated with it, we used two alternative methods. First, for completeness, we used the same method as the deep water end members (first 4 rows, Table S5). Assuming that DIC drawdown by phytoplankton (above 15 m) may not be well-captured by this simple method, we also took each summer profile (8) from that region and integrated S and DIC in the top 15 m (same method as for water column inventories, Text S3; Table S6). We summarized these results by computing the mean S and DIC of the 8 integrations (Row 5, Table S5).

Mixing-line comparisons: Equations for DIC-S mixing-lines defined by shallow (FR-plume) and deep end-members were computed. Any point in DIC-S space that lies within the S-range spanned by two end-members and above the mixing-line defined by the same end-members is carbon-rich relative to a mix of those two end-members.

Extrapolation of DIC mixing lines determined by the FR-plume and any of the potential deep end-members to S=0 provide insight into the DIC contribution of the pure FR end-member. Biological DIC draw-down in the FR-plume will make that intercept smaller by pulling down the FR-plume end-member. Remineralization, production of DIC, in the deep (higher S) water masses will also make the intercept smaller. Thus, positive DIC intercepts (S=0) indicate a strong FR DIC contribution.

References

Barwell-Clarke, J., and F. Whitney (1996), Institute of ocean sciences nutrient methods and analysis, *Can. Tech. Rep. Hydrogr. Ocean Sci.*, *182*, vi + 43pp.

Bylhouwer, B., D. Ianson, and K. Kohfeld (2013), Changes in the onset and intensity of wind-driven coastal upwelling and downwelling along the North American Pacific coast, *J. Geophys. Res.*, *118*, 1–16, doi:10.1002/jgrc.20194.

Carpenter, J. H. (1965), The Chesapeake Bay Institute technique for the winkler dissolved oxygen method, *Limnol. Oceanog.*, *10*, 141–143.

Clayton, T. D., and R. H. Byrne (1993), Spectrophotometric seawater pH measurements: total hydrogen ion concentration scale calibration of m-cresol purple and at-sea results, *Deep Sea Res. I*, *40*, 2115–2129.

Dewey, R. (2012), VENUS observes robust annual cycles, with slightly cooler 2011, in *State of the physical, biological, and selected fishery resources of Pacific Canadian marine ecosystems in 2011.*, *Canadian Science Advisory Secretariat, Research Document*, vol. 2012/072, edited by J. R. Irvine and W. R. Crawford, pp. 102–104, Fisheries and Oceans Canada.

Dickson, A. G., C. L. Sabine, and J. R. Christian (2007), *Determination of dissolved organic carbon and total dissolved nitrogen in sea water*, PICES Special Publication 3.

Friis, K., A. Krtzinger, and D. W. R. Wallace (2003), The salinity normalization of marine inorganic carbon chemistry data, *Geophysical Research Letters*, *30*(2), doi:10.1029/2002GL015898.

Garcia, H. E., and L. I. Gordon (1992), Oxygen solubility in seawater: Better fitting equations, *Limnol. Oceanog.*, *37*(6), 1307–1312.

Garcia, H. E., and L. I. Gordon (1993), Erratum: Oxygen solubility in seawater: Better fitting equations, *Limnol. Oceanog.*, *38*(3), 656.

Ho, D. T., C. S. Law, M. J. Smith, P. Schlosser, M. Harvey, and P. Hill (2006), Measurements of air-sea gas exchange at high wind speeds in the southern ocean: Implications for global parameterizations, *Geophys. Res. Lett.*, *33*(16).

Hunt, C. W., J. E. Salisbury, and D. Vandemark (2011), Contribution of non-carbonate anions to total alkalinity and overestimation of pCO_2 in New England and New Brunswick rivers, *Biogeosciences*, *8*, 30693076, doi:10.5194/bg-8-3069-2011.

Masson, D. (2002), Deep water renewal in the Strait of Georgia, *Est. Coast. Sh. Sci.*, *54*(1), 115 – 126, doi:10.1006/ecss.2001.0833.

Masson, D. (2006), Seasonal water mass analysis for the Straits of Juan de Fuca and Georgia, *Atmos. Ocean*, *44*, 1–15.

Millero, F. J. (1979), Thermodynamics of the carbonate sytem in seawater, *Geochim. Cosmochim. Ac.*, *43*(10), 1651–1661.

Millero, F. J. (2010), Carbonate constants for estuarine waters, *Mar. Fresh. Res.*, *61*(2), 139–142, doi:10.1071/MF09254.

Moore-Maley, B. L., S. E. Allen, and D. Ianson (2016), Locally driven interannual variability of near-surface pH and Ω_A in the Strait of Georgia, *J. Geophys. Res.*, *121*, doi:10.1002/2015JC011118.

Riche, O. G. J., and R. Pawlowicz (2014), Variability in a fjord-like coastal estuary I: Quantifying the circulation using a formal multi-tracer inverse approach, *Est. Coast. Sh. Sci.*, *137*, 1–13, doi:10.1016/j.ecss.2013.11.018.

Riley, J. P., and M. Tongudai (1967), The major cation/chlorinity ratios in sea water, *Chem. Geol.*, *2*, 263–269.

Sutton, J. N., S. C. Johannessen, and R. W. Macdonald (2013), A nitrogen budget for the Strait of Georgia, British Columbia, with emphasis on particulate nitrogen and dissolved inorganic nitrogen, *Biogeosci.*, *10*, 71797194, doi:10.5194/bg-10-7179-2013.

UNESCO (1981), The practical salinity scale 1978 and the international equation of state of seawater 1980, *Tech. Pap. Mar. Sci.*, *36*, 1–25.

van Heuven, S., D. Peirrot, J. Rae, E. R. Lewis, and D. W. R. Wallace (2011), *MATLAB program developed for CO_2 System Calculations*, DOE (U.S. Department of Energy), Oak Ridge National Laboratory, Tennessee, ORNL/CDIAC-105b.

Wanninkhof, R. (1992), Relationship between gas exchange and wind speed over the ocean, *J. Geophys. Res.*, *97*(C5), 7373–7382.

Wanninkhof, R., W. E. Asher, D. T. Ho, C. Sweeney, and M. W. R. (2009), Advances in quantifying air-sea gas exchange and environmental forcing, *Annu. Rev. Mar. Sci.*, *1:213-44*, doi:10.1146/annurev.marine.01,908.163,742.

Weiss, R. (1974), Carbon dioxide in water and seawater. The solubility of a non-ideal gas, *Mar. Chem.*, *2*, 203–215.

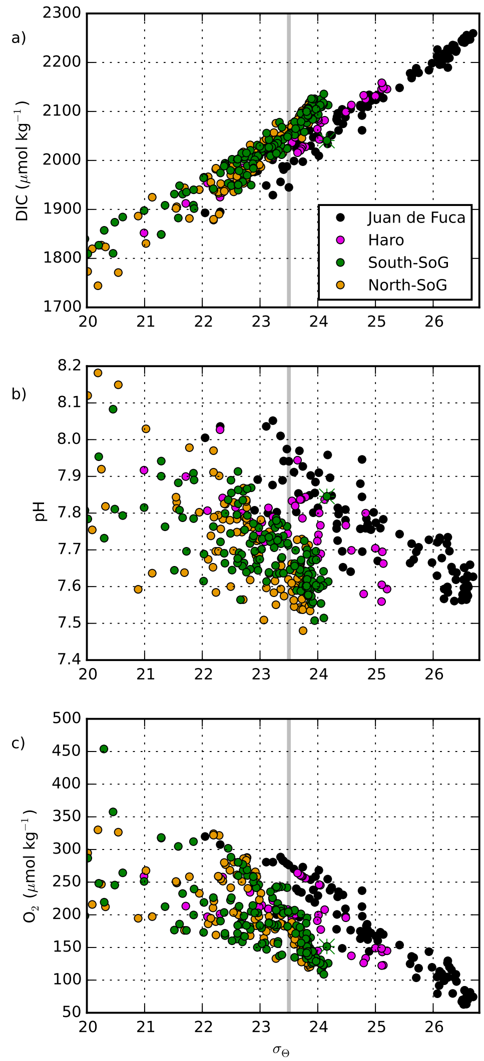

Figure S1. DIC (a), pH (b), and O_2 (c) as a function of σ_θ for all discrete data coloured by region. Measurement uncertainty in DIC (a) and O_2 (c) is smaller than the diameter of the symbols. Uncertainty in pH (estimated from DIC and TA) is < 0.036, $S > 31$; < 0.038, $26 < S < 31$. The grey vertical line indicates a salinity of 30.3 ($\sigma_\theta \sim 23.5$) associated with the water entering the SoG from Haro Strait ($\sim$ 100 m depth). A deep water intrusion from the Haro region to the S-SoG on 16 July 2012 (Figure S2) is shown with a green star.

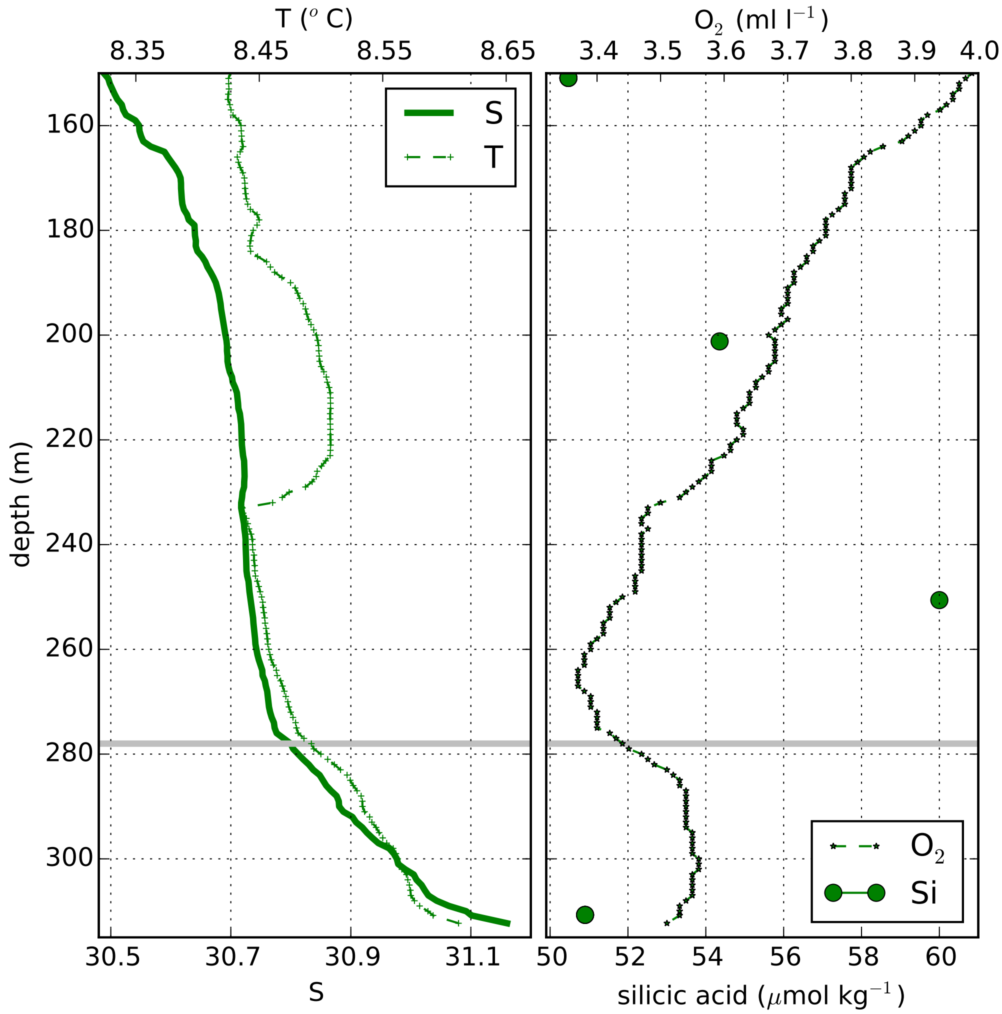

Figure S2. Vertical salinity (S), temperature (T), (left panel) O_2 and $Si(OH)_4$ (right panel) profiles collected on 16 July 2012 (cruise 2012-57) in the S-SoG (49.02 °N, 122.57 °W). S, T and O_2 were measured by the CTD with O_2 sensor, while the $Si(OH)_4$ was analyzed from discrete Niskin bottles. These profiles illustrate a deep water intrusion of water from Haro Strait roughly 30 m thick, below 280 m (increased S, T, O_2, and decreased macro-nutrients - and DIC - see Figure 2a). Such events are common in the S-SoG during summer, occurring once or twice per month following neap tides [*Masson*, 2002; *Dewey*, 2012]. Later in the summer they often cause a decrease in O_2. The passage of water from Haro to the mid S-SoG (49°N) takes only 3 d in this event. Our data show no evidence of similar intrusions in the N-SoG.

Table S1. Chronological list of all cruises (cruise ID – year-#) in the Northern Salish Sea and the dates during which carbon data were collected. The full Masson/Chandler program [*Masson*, 2006] includes the Straits of Juan de Fuca (J), Haro (H) and Georgia (SoG) (Figure 1a). In this study, the SoG is divided into two zones; the south (S) and the north (N). Regions in which carbon data were collected are included in the third column. The Johannessen program [*Sutton et al.*, 2013] sampled one station in the northern SoG and one in the southern SoG. The Ianson cruise, a single large-scale survey devoted to studying ocean acidification, sampled only two sites in the Salish sea. Where cruise ID have a * discrete pH were collected in addition to dissolved inorganic carbon (DIC) and total alkalinity (TA).

cruise ID	dates	regions	program
2003-29	Sep 2 – 4	H J	Masson/Chandler
2003-41	Dec 2 – 4	S H J	Masson/Chandler
2010-16	Apr 5	N S	Johannessen
2010-36*	Jul 21	S J	Ianson
2010-57	Aug 6 – 7	N S	Johannessen
2010-73	Oct 30 – 31	N S	Johannessen
2011-28	Apr 5 – 6	N S	Johannessen
2011-09*	Jun 22 – 24	N S H J	Masson/Chandler
2011-60	Aug 6 – 7	N S	Johannessen
2011-10*	Sep 10 – 13	N S H J	Masson/Chandler
2011-76	Nov 25 – 27	N S	Johannessen
2012-19	Apr 2 – 3	N S	Johannessen
2012-04	Apr 6 – 9	N S H J	Masson/Chandler
2012-05	Jun 14 – 17	N S H J	Masson/Chandler
2012-57	Jul 15 – 16	N S	Johannessen
2012-06	Sep 20 – 23	N S H J	Masson/Chandler

Table S2. Seasonal partitions determined by typical downwelling, upwelling and transition seasons estimated from winds on the outer coast of Vancouver Island [*Bylhouwer et al.*, 2013], or in the case of 'freshet', by surface salinity in the S-SoG. The freshet defined here is a subset of the summer season and occurs only during years of strong Fraser River flow.

Season	timing	# cruises	stations [a]			
			J	H	S	N
winter	November – February	2	4	1	2	1
spring	March – mid-May	4	3	1	4	5
freshet	south-SoG surface S $<$ 20	4	3	2	5	5
summer	mid-May – September	5	8	3	4	2
fall	October – November	1	0	0	1	1

[a] Number of stations sampled in each region; J = JdF, H = Haro, S = S-SoG, N = N-SoG

Table S3. Tidal phase (observed at Pt. Atkinson just north of the mouth of the Fraser River (49.33°N, 123.26°W); max tidal range $\sim$ 5 m) and wind speed on days when Haro Strait was sampled, ordered from spring to winter. Cruise identification (ID) (year-#) is followed by date of sampling. Tidal phase is described relative to neap and spring tides (a and f indicate approaching and following, respectively) with the approximate height of the tidal envelope on the day preceding data collection. The mean and variance of the hourly wind speed collected in the S-SoG near the mouth of the Fraser River (Sandheads - http://climate.weather.gc.ca/) was computed over the 5 days straddling sample collection. All Haro samples were collected at the same location, roughly in the middle of the Haro region (48.63°N, 123.24°W) with the exception of 2003-41* which was sampled just north (48.77°N, 123.03°W) at the entrance to S-SoG (Figure 1a).

cruise ID	date	tides (m)	5-day winds mean, var (m/s)
2012-04	Apr 6	f-neap: 2.0	5.8, 3.2
2011-09	Jun 22	a-neap: 2.5	4.0, 2.0
2012-05	Jun 14	f-neap: 2.0	4.3, 2.0
2003-29	Sep 2	mix: 3.0	7.1, 3.6
2011-10	Sep 10	mix: 3.0	5.0, 2.4
2012-06	Sep 20	a-spring: 3.5	5.4, 2.7
2003-41*	Dec 2	a-neap: 2.5	5.6, 2.6

Table S4. Estimated total inventories (Inv_T) for DIC and O_2 in Haro Strait (section 2.2) are ordered from spring to winter. Inv_d is the inventory of inorganic carbon supersaturation and O_2 undersaturation throughout the water column in Haro Strait (d - disequilibrium); i.e. for DIC, $\mathrm{Inv}_d = \mathrm{Inv}_T$ - Inv_e; for O_2, $\mathrm{Inv}_d = \mathrm{Inv}_e$ - Inv_T, where Inv_e is the equilibrium inventory. Surface level of O_2 saturation, sΔO_2 is defined as (O_{2m}/O_{2e} - 1)×100, where m and e indicate measured and equilibrium surface concentrations, respectively. (sΔDIC = (sP_{CO2}/aP_{CO2} - 1)×100 where P_{CO2} is the partial pressure of carbon dioxide and s and a represent surface ocean and atmospheric, respectively.) Gas flux is the total gas flux occurring over the period of 5 days straddling the sampling date in the Haro region (Text S3; Table S3). X is the fraction of Inv_d that is erased by the 5 day gas flux (Text S3). All Haro samples were collected at the same location, roughly in the middle of the Haro region (48.63°N, 123.24°W, depth 233 m) with the exception of 2003-41* which was sampled just north (48.77°N, 123.03°W, depth 214 m) at the entrance to S-SoG (Figure 1a).

cruise ID	Inv_T (mols)		Inv_d (mols)		s Δ (%)		Gas flux (mols)		X (%)	
year-#	DIC	O_2	DIC	O_2	DIC	O_2	DIC	O_2	DIC	O_2
2012-04	6.0e11	7.4e10	1.8e10	1.4e10	23	-12	7.1e7	5.7e8	0.4	4.1
2011-09	6.2e11	4.9e10	2.9e10	3.6e10	90	-25	1.4e8	6.3e8	0.5	1.8
2012-05	6.1e11	5.3e10	3.2e10	3.2e10	55	-10	9.4e7	2.9e8	0.3	0.9
2003-29	6.0e11	4.9e10	1.6e10	3.3e10	8	-26	3.3e7	1.8e9	0.2	5.5
2011-10	6.1e11	4.3e10	3.4e10	3.3e10	41	-23	8.9e7	8.7e8	0.3	2.1
2012-06	6.1e11	4.4e10	3.1e10	4.0e10	74	-27	1.8e8	1.2e9	0.6	3.0
2003-41*	5.5e11	5.6e10	2.1e10	2.3e10	29	-14	7.7e7	6.3e8	0.3	2.0

Table S5. Inorganic carbon end-members for major water masses in the SoG in summer. During other seasons the water masses have different properties [*Masson*, 2006] (M06). Bold S are M06 summer end-members (rows 1–4); we call the M06 'river' end-member 'FR-plume'. Adjacent DIC values were estimated from our DIC data (std = standard deviation; n = number of data) in the salinity range used (col 6) in the given region (Text S4). To avoid bias, the FR-plume end-member was also estimated from averaging S and DIC in the upper 15 m (following M06) in all available summer and freshet profiles (Text S4; Table S6), summarized in Row 5. The vertical distance between the mixing-line defined by the *d*JdF and FR-plume(b) end-members and the points in DIC-S space defined by the other end-members ($\Delta DIC_{FR(b):JdF}$) is given in the final column.

end-member	S (PSS-78)	DIC (μmol kg^{-1}) mean	std	n [a]	S-range	$\Delta DIC_{FR(b):JdF}$ (μmol kg^{-1})
deep JdF	**33.9**	2250	4	20	S > 33.8	0
deep S-SoG	**31.0**	2110	11	11	30.8 < S < 31.2	+20
deep N-SoG	**30.5**	2090	12	26	30.3 < S < 30.7	+25
FR-plume	**25.1**	1760	13	4	24.1 < S < 26.1	-10
FR-plume [b]	23.2	1670	120	8	18.6 – 26.6	0

[a] n = number of data in chosen S-range (rows 1-4); in rows 5-6, n = number of profiles.

[b] Mean result of integrating top 15 m of all summer and freshet S-SoG profiles (Text S4; Table S6).

Table S6. Average S (PSS-78) and DIC (μmol kg^{-1}) in the top 15 m of the water column (col 2 and 3, respectively) for all profiles with sufficient data (at least two) in that zone during the summer and freshet season (Table S2) in the S-SoG adjacent to the mouth of the Fraser River (3 locations, Figure 1a) to determine the Fraser River end member *sensu Masson* [2006]. The DIC value (μmol kg^{-1}) at S = 30.13 [a] that lies on the mixing-lines resulting from the potential FR-plume end-member and the *d*Jdf and *d*S-SoG end-members (Table S5), respectively was estimated (cols 4, 5). Data from the profile associated with Figure 3c and d are in bold font. Freshet profiles are indicated by a *. Data are ordered chronologically with cruise ID (Table S1).

cruise ID	S	DIC	mixing-line DIC(S=30.13) w/*d*JdF	w/*d*S-SoG	date
2010.36	**26.33**	**1760**	**2006**	**2045**	**21 July 2010**
2011.09*	22.12	1666	2063	2067	24 Jun 2011
2011.60*	20.63	1542	2049	2062	7 Aug 2011
2011.10	24.56	1652	2009	2048	11 Sep 2011 (stn 42)
2011.10	25.21	1703	2013	2049	12 Sep 2011 (stn 39)
2012.05*	18.56	1532	2074	2069	16 June 2012
2012.57*	21.99	1599	2043	2061	16 July 2012
2012.06	26.58	1833	2035	2055	22 Sept 2012

[a] An arbitrary salinity that falls between the S associated with all deep end-members and the S of all potential FR-plume end-members was chosen. The minimum Ω_a from the single (21 July 2010) profile shown in Figure 3c has S = 30.13; DIC = 2027μmol kg^{-1}.